Mass Transfer from Dispersed Bubbles to Electrolyte Solution in Packed Beds

The measurement of gas-liquid interfacial areas and mass transfer coefficients in concurrent upward bubbly flow (u_G from 0.02 to 0.16 m/s, u_L from 0.0051 to 0.056 m/s) over a packed bed consisting of 1.2 mm glassy carbon particles is described. Specific surface areas were measured by chemical absorption of O_2 into Na_2SO_3 solutions; volumetric mass transfer coefficients were measured by physical desorption of O_2 into N_2 bubbles. Surface areas were obtained in the range of 4×10^3 to 2×10^5 m^{-1}, much higher than have been previously reported. High areas are related to the use of electrolytes and small packing particles. Bubble size was found to depend primarily on liquid velocity. Volumetric mass transfer coefficients $k_L a_G$ are also high ($0.1 < k_L a_G < 2.3$ s^{-1}), primarily as a result of high gas-liquid interfacial areas. Mass transfer coefficients k_L are small, however. For the smaller bubble dispersions, mass transport is controlled by diffusion rather than by convection.

Ken M. Takahashi,
Richard C. Alkire
Department of Chemical Engineering
University of Illinois
Urbana, IL 61801

Introduction

Gas-liquid electrochemical reactors typically have high surface area porous electrodes, through which the two-phase electrolyte flows. In such reactors, the pore size is sufficiently small that conventional scaling arguments are not adequate for extrapolating mass transfer data from classical chemical engineering operations on large packings. In this study, gas-liquid interfacial area and mass transfer characteristics of dispersed-bubble flow through packed beds of small particles are investigated.

The packing material and solutions used in this study are characteristic of those employed for the electrochemical oxidation or reduction of gaseous species. Typically, in such systems, the gaseous reactants are only sparingly soluble in aqueous electrolyte solutions. As a consequence, the rate of mass transfer between phases tends to be slow and thus limits the performance of such reactors. Ultimately, the gaseous species must gain or lose electrons, either directly via electrochemical reaction at the particle surfaces, or indirectly via homogeneous reaction with dissolved redox couples that are, in turn, regenerated by electrolysis. In either case, interfacial area and mass transfer data are needed to design such electrochemical systems.

This study is part of a broader project aimed at the prediction of current distribution and reaction selectivity in porous electrodes that employ dissolved redox catalysts and gas-liquid flow. The successful development of such reactors could exert a significant impact on the use of oxygen electrodes in chlorine electrolyzers, fuel cells, and many electro-organic synthesis processes.

Reactors that employ the transfer of reactant from gas to liquid and thence to a reactive particle surface generally require small particles. Examples of such reactors include hydrodesulfurization reactors (Van Deemter, 1964; Lister, 1964), catalytic SO_2 oxidizers (Goto et al., 1977), oxygen electrodes for the production of hydrogen peroxide (Oloman and Watkinson, 1976, 1979), packed bed electrodes for alkene epoxidation (Ellis and Jansson, 1983) and recovery of metal ions (Ehdaie et al., 1982).

A rich literature on mass transfer in phase contacting operations has been reviewed by Charpentier (1976, 1981), Sweed (1981), and Hofmann (1978). Charpentier (1976) suggested that a cut-off between large and small particles lies in the neighborhood of 3 mm, below which attempts to apply unifying correlations have failed. Uncertainty about the behavior of small-particle systems is compounded by the scarcity of experimental data in these systems.

Both gas-liquid surface area (a_G) and mass transfer coefficients (k_L) depend on bubble size. While motion of large bubbles with respect to the surrounding liquid is affected primarily by bouyant convection and inertia, small bubble motion is more sensitive to surface forces such as surface tension, viscous drag, and electrostatic repulsion. The bubble-size distribution in flow-through packed beds represents a steady-state balance between

---

Present address of K.M. Takahashi: AT&T Bell Laboratories, Murray Hill, NJ 07974.

breakup and coalescence of bubbles, each of which is a poorly understood phenomenon. In the study of the breakup of liquid droplets and bubbles, Hinze (1955) found that for most flows, a critical Weber number exists, below which a stable dispersion can be achieved in the absence of coalescence. The stable bubble size depends on the characteristic liquid shear stress and decreases with decreasing packing size. When bubble dispersions are concentrated, coalescence also plays an important role. The properties of a thin liquid film, which separates bubbles, determine the likelihood of coalescence. Fluid drainage causes the film to thin until it becomes unstable owing to the effects of electrostatic forces and London-van der Waals forces (Miller, 1978). Factors which slow film drainage such as surfactants, impurities, and streaming potentials, will thus inhibit coalescence (Brandon et al., 1985). The presence of electrolytes in the liquid phase serves to inhibit coalescence (Lessard and Zieminski, 1971) and dramatically to decrease bubble size in concentrated swarms (Zieminski and Whittemore, 1971).

Because surface effects have a strong influence on bubble flow over small particles, hydrodynamics and mass transfer show a complex dependence on gas, liquid and solid composition. Most data on bubble specific surface area (a_G) during flow through small packings have been obtained from chemical absorption of CO_2 into NaOH solutions. Saada (1972) measured a_G for flow over glass beads (0.5, 1.0 and 2.1 mm diameter; liquid velocity, 0.019 to 0.059 m/s; gas velocity, 0.034 to 0.56 m/s), and found specific surface areas that ranged from 250–900 m^{-1}. In the gas-continuous regime, a_G was found to be insensitive to gas velocity. In general, the gas-liquid specific surface area was much less than the specific surface area of the solid particles that comprised the packed bed. The data reported by Voyer and Miller (1968) for CO_2 absorption into NaOH solution in flow over packings consisting of cylinders of six mesh stainless steel cylindrical screens include some velocities which were comparable to those of Saada ($0.005 < u_L < 0.032$, $0.09 < u_G < 0.82$ m/s); the measured gas-liquid specific surface areas were comparable to those reported by Saada for the same velocities.

Ohshima et al. (1976), measured a_G for flow over beads (1, 2.8 and 4.3 mm dia.) using O_2 absorption in Na_2SO_3 solutions. However, as a result of fluidization of the small particles under most flow conditions, the low values of a_G they reported are not representative of flow over fixed beds of small particles.

Literature values of $k_L a_G$ for cocurrent upward gas-liquid flow over small packings are generally in fair agreement. In addition to a_G measurements, Saada (1972) measured the product $k_L a_G$ for the same range of flows and proposed for gas-continuous flow:

$$Sh_G = 10.3\, Re_G^{0.09}\, Re_L^{0.58} (d_p/d_t)^{0.34} \tag{1}$$

and for bubbly flow:

$$Sh_G = 10.7\, Re_G^{0.22}\, Re_L^{0.32} (d_p/d_t)^{0.33} \tag{2}$$

The $k_L a_G$ data of Voyer and Miller (1968) fell roughly within the same range as those of Saada for comparable fluid velocities. Goto et al. (1975), used O_2 absorption from pure water to measure $k_L a_G$ for flow over CuO/ZnO particles (0.54 to 2.4 mm dia.). Velocities were low ($4 \times 10^{-4} < u_L < 6 \times 10^{-3}$, $2 \times 10^{-3} < u_G < 8 \times 10^{-3}$ m/s) so direct comparison with other data was not possible. Goto and coworkers (1975) extrapolated the correlations of Saada to their own conditions of study and found only fair agreement. The primary difference between the two studies is that Saada used glass particles while Goto used CuO/ZnO particles. Probably as a result of differing packing material, Goto observed flows that were bubbly, not gas-continuous as predicted by Saada.

Understanding of the factors that influence fluid flow in packings made of small particles is currently insufficient to correlate flow phenomena to physical properties. In particular, insufficient data are available in small-particle beds to elucidate the effects of electrolytes and of particle wettability. The purpose of this study was to measure the gas-liquid area and mass transfer coefficients of cocurrent upward flow in a particular small-particle system. Results show that the electrolyte solutions and small-particle packings of this study create very fine bubble dispersions, with specific areas much higher than have been reported previously. The high areas provide rapid mass transfer, even though mass transfer from the finer dispersions is shown to be diffusion-controlled.

Experimental Apparatus and Procedure

Mass transfer coefficient and interfacial G-L surface area measurements were made in packed beds of rectangular cross section (width of 2.4 cm, thickness 0.6 cm). One face of cells containing the packed beds was transparent to allow observation of the flow. The length of packing in the direction of flow was varied from 4 to 10 cm. The packing consisted of 1.2 mm dia. glassy carbon particles (Gulf General Atomic Corp., San Diego), with a specific surface area of 3,300 m^{-1}. The packing material was nonporous and electrically-conductive properties that make it ideal for electrochemical applications, particularly for fundamental studies, for which precise knowledge of surface area is important.

Aqueous solutions were recirculated through the cell via a 4 lit. reservoir, in which dissolved gas (Union Carbide, Linde Division) concentrations were maintained by bubbling. Gas bubbles were introduced at the bottom of the packed bed through four 22 ga. capillary tubes which were evenly spaced across the packing width. Solutions were prepared from deionized water and reagent grade chemicals. Gas and liquid phases were held at temperatures near 27°C, and were maintained at 1 atm pressure at the cell exit.

Interfacial Area Measurements

In a manner similar to that described by deWaal and Okeson (1966), gas interfacial area was measured by absorption of oxygen, from a mixture of 10% oxygen/90% nitrogen, into a Na_2SO_3 solution, where the reaction $O_2 + 2\,SO_3^{-2} \rightarrow 2\,SO_4^{-2}$ occurred. The sulfite concentration decayed from its initial value of 1.2 M to as low as 0.6 M during the course of several dozen sampling cycles. The oxidation product was considered to be solely Na_2SO_4. To catalyze the reaction, 1×10^{-4} M $CoSO_4$ was added and the pH was adjusted to 8.5.

Specific area calculations were based on the change in O_2 concentration in the gas phase between the cell inlet and outlet. Gas was sampled at the cell exit through a vertical sample port that could be filled with two-phase mixture at the packing exit composition. Gas samples were analyzed on a Varian 3700 gas chromatograph, in which the 60/80 mesh molecular sieve 5A column was held at 40°C.

The reaction rate constant was measured with the gas burette method, in which the rise of soap film in a burette was used to determine absorption rate. The reaction vessel was a cylindrical container which held samples of about 500 mL of sulfite solution. Gas and liquid phases were agitated with a small fan and stir ball, respectively, which did not cause appreciable disturbance of the liquid surface. Rate calculations were thus based on the geometric area of 0.0158 m^2. Additional details on cell construction and procedure are available (Takahashi, 1986).

Mass Transfer Measurements

Gas-liquid mass transfer rates were measured by desorption of oxygen from an air-saturated 0.70 M Na_2SO_4 solution into nitrogen bubbles. The solution in the reservoir was held near saturation by vigorous bubbling with air. The packed bed used for mass transfer measurements was identical to the cell used for area measurements except that it had a large downstream chamber for separation of gas and liquid flows. Inlet and outlet concentrations of oxygen in the liquid phase were measured with an oxygen probe (LAZAR DO 166), and were used to calculate the mass transfer coefficients. Cell inlet concentrations were measured by pumping the liquid through the cell and past the oxygen probe in the absence of nitrogen flow. For outlet measurements in the presence of gas-liquid flow, the phases were separated in the chamber and the liquid phase was passed over the oxygen probe.

Results and Discussion

Existing literature on the flow of bubble dispersions suggests that when either bubbles or their flow channels are small, interfacial phenomena play key roles in the determination of fluid flow patterns and thus of gas-liquid mass transfer rates. The size distribution of concentrated bubble dispersions depends on the facility of coalescence, which for small bubbles is influenced strongly by the presence of surfactants and electrolytes. In addition, confined flow channels force bubbles into close contact with the channel walls. The wettability of the solid surface is therefore expected to have a strong effect on flow patterns in these systems.

In this study, the packing thickness (0.6 cm) corresponded to five particle diameters, a choice which made possible additional electrochemical studies that are reported elsewhere (Takahashi, 1986). As a consequence, however, edge effects may have influenced the results of this study to a small extent. Nevertheless, the very fine bubbles reported below are dramatically different from those previously observed in small particle systems owing to the presence of electrolyte in the solution. Edge effects, if present, would be expected to be minor by comparison with differences from other investigations owing to the electrolyte and small packing effects studied here.

Interfacial Area Measurements

The oxidation of sulfite to sulfate involves a multistep free radical mechanism (Backstrom, 1934), and the apparent reaction order therefore depends on reaction conditions. The reaction is zero order in sulfite when the sulfite concentration greater than 0.4 M, as established by de Waal and Okeson (1966) under conditions of convective chemical absorption of oxygen. Gas-liquid mass transfer rates in this study were at all times such as to prevent the interfacial concentration of sulfite from dropping below the 0.4M threshold value.

Linek and Mayrhoferova (1970) demonstrated that the reaction is second order in oxygen when the dissolved oxygen concentration is less than 6×10^{-4} M. For 1.2 M salt solutions, this means that O_2 absorption is second order for oxygen partial pressures up to about 1 atm, a criterion satisfied in this study.

For (0, 2) order kinetics, the absorption flux is given by

$$N = (C^{\text{sat}})^{3/2} \sqrt{2k_r D/3} \tag{3}$$

Absorption flux measured by the gas burette method can be used to calculate the second order rate constant:

$$k_r = \frac{3N^2}{2(C^{\text{sat}})^3 D} \tag{4}$$

The measured rate constant was $(3.25 \pm 0.45) \times 10^6$ m^3/kmol · s (95% confidence) for an average temperature of 26.6°C, a pH value of 8.5, $CoSO_4$ concentration of 1×10^{-4} M, and a sulfite concentration ranging from 0.6 to 1.1 M as determined by iodometric titration (Vogel, 1961). Oxygen solubility from air was considered to be comparable to its value of 9.61×10^{-5} M at 26.6°C in 1.2 M Na_2SO_4 (Battino, 1981). Oxygen diffusivity was approximately 1.2×10^{-9} m^2/s based on the data of Davis *et al.* (1967) for 1 M KOH solution and corrected for viscosity by the Nernst-Einstein equation. The rate constant reported here was 28% lower than the value (4.5×10^6 $m^3 \cdot$ s) obtained by extrapolation from data of Linek and Mayrhoferova (1970).

When plug flow exists within the packed bed, the variation in O_2 concentration in the gas phase in the direction of flow is given by:

$$-u_G\, dC = N\, a_G\, dx \tag{5}$$

Combination of Eqs. 3 and 5 results in an expression for bubble area as a function of inlet and outlet concentration of oxygen in the gas phase:

$$a_G = \frac{u_G \sqrt{6}\,(\sqrt{C_{G,0}/C_{G,\ell}} - 1)}{\ell \sqrt{r_c^3\, k_r D C_{G,0}}} \tag{6}$$

The variable ℓ is the packed bed length, and r_c is the ratio of oxygen solubility in the liquid phase to the gas phase oxygen concentration (i.e., a dimensionless Henry's Law constant). O_2 absorption in the withdrawal port prior to sampling was negligible for $a_G > 10^4$ m^{-1}. Correction of low-area data for this effect is described elsewhere (Takahashi, 1986).

Specific gas areas were measured in flows having a liquid velocity between 8.1×10^{-3} and 5.6×10^{-2} m/s and a gas velocity between 2.0×10^{-2} and 1.6×10^{-1} m/s. For the few data taken at liquid velocities less than 1.5×10^{-2} m/s, flows were observed to approach the gas-continuous regime (Takahashi and Alkire, 1985). Most data were taken at higher u_L values, for which the flows were bubbly; under such conditions, the bubbles were smaller than the packing particles, and for high gas and liquid flow rates, were extremely small. It was therefore expected that a_G values much greater than the packing area (3,300 m^{-1}) should be measured.

Bubble interfacial area data are shown in Figure 1 for a range of liquid and gas flow rates. Gas areas were found to depend linearly on gas velocity, and had values that were much higher than the packing area. The linear dependence on gas flow may indicate that increasing the gas velocity changes the number of bubbles present, more than the distribution of size. A relative insensitivity of bubble size to gas flow rate had been observed previously (Takahashi and Alkire, 1985). To describe the results in Figure 1 for later calculations, the data were correlated by the expression:

$$a_G(\mathrm{m}^{-1}) = 4{,}680 + [(1.41 \times 10^8)u_L^{1.72} + (1.65 \times 10^5)]\, u_G \quad (7)$$

which is compared with experimental data in Figure 2. Equation 7 shows that the area (and therefore the bubble size) strongly depended on liquid velocity.

The areas measured in this study were much higher than those observed by Saada (1972) in 0.1–0.5 M NaOH solutions and by Voyer and Miller (1968) in 1.0 M NaOH Solution. The difference is in accord with the visual observation that bubbles generated in 1 M NaOH by the packed bed were much larger than those in the sulfite/sulfate solution used in the present study. In the sulfite/sulfate solutions, bubbles much smaller than the particles could be seen; accordingly, the small bubbles gave higher interfacial areas. The difference in surface tensions of the two solutions is less than 2% and does not explain the effect. The dominant effect of salt on bubble size is probably the inhibition of bubble coalescence by electrolyte observed by Lessard and Zieminski (1971).

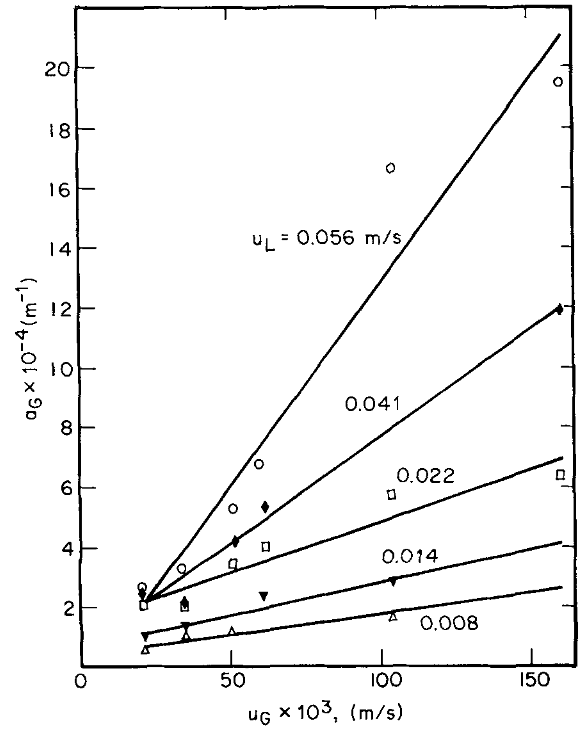

Figure 1. Gas-liquid interfacial area in the flow range 2.0 × $10^{-2} < u_G < 1.6 \times 10^{-1}$ m/s and 8.1 × $10^{-2} < u_L < 5.6 \times 10^{-2}$ m/s.

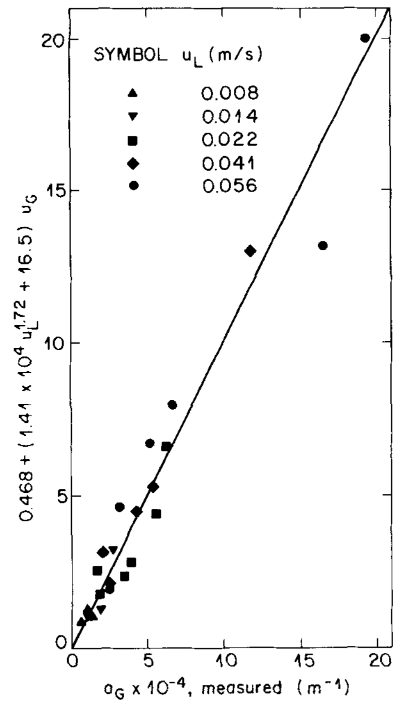

Figure 2. Gas-liquid area correlation.

By assuming that the bubbles are spherical and uniform in size, a mean bubble diameter can be estimated:

$$d_b = \frac{6}{a_G} \epsilon \beta_G \quad (8)$$

where $\epsilon\beta_G$ is the total gas fraction in the cell. Under flow conditions similar to those of this study, gas holdup β_G is generally in the range of 0.5 to 0.9. If $\epsilon\beta_G$ is assumed to be around 0.3, based on a random-packing void fraction (ϵ) of 0.4 and gas holdup of approximately 0.8, a dispersed bubble area range of 1 × 10^4 to 2 × 10^5 m^{-1} corresponds to a size range of 200 to 10 μm. Therefore, at low velocities bubbles are nearly as large as packing voids, while under high flow conditions, 10 μm bubbles can exist. It should be mentioned that bubble size was by no means uniform. Even for the high area flows, large bubbles (>100 μm) could be seen among the smaller ones. It is reasonable to assume, then, that bubbles smaller than 10 μm provide a significant area contribution. By comparison, Fukui and Yuu (1985) found that bubble size followed a log-normal distribution, with a most probable bubble size around 10 μm for electrogenerated bubbles in sodium sulfate solutions.

Mass Transfer Measurements

When oxygen is desorbed from an air-saturated solution into nitrogen gas, the composition of both phases changes at a rate that is proportional to the local concentration driving force ($C^{sat} - C_L$) times the volumetric mass transfer coefficient $k_L a_G$. Because gas-phase concentrations and diffusivities are much higher than those in the liquid phase ($C_G/C_L = 1/r_c \approx 100$, $D_G/D_L \approx 10^4$), gas phase mass transfer resistance is negligible. A differential mass balance based on the assumption of plug flow gives $k_L a_G$ as a function of inlet (C_o) and outlet (C_ℓ) concentrations of oxygen in the liquid phase:

$$k_L a_G = \frac{u_L}{\ell}\left(\frac{1}{1+\frac{r_c u_L}{u_G}}\right)\ln\frac{u_G/r_c u_L}{\left(1+\frac{u_G}{r_c u_L}\right)\frac{C_\ell}{C_o}-1} \tag{9}$$

where ℓ is the packed bed length. When C_ℓ can be measured precisely, Eq. 9 can be used to determine $k_L a_G$ values. Under most flow conditions, however, the cell effluent consisted of finely dispersed bubbles. As a result, phase separation in the exit chamber was not immediate. Correction for absorption in the post-cell disengagement region was described by Takahashi (1986). Because extreme gas and liquid velocities resulted in the flow of two-phase dispersion beyond the cell, the usable range of flow was limited to the ranges $5.1 \times 10^{-3} < u_G < 5.1 \times 10^{-2}$ and $2.1 \times 10^{-2} < u_L < 5.1 \times 10^{-2}$. Mass transfer results within this range appear in Figure 3. The data are correlated by:

$$\ln(k_L a_G) = 73.5\, u_G + 32.4\, u_L - 3.49 \tag{10}$$

which is compared with $k_L a_G$ data in Figure 4. Figure 3 and Eq. 10 show that, unlike a_G values, $k_L a_G$ is more strongly influenced by gas than liquid velocity. The $k_L a_G$ values in this study (0.1 to 2.3 s^{-1}) are higher than those measured by other authors (Saada, 1972; Voyer, 1968), in NaOH solutions, and reflect the very high gas-liquid specific areas encountered in this study.

If very small bubbles exist, perhaps smaller than 10 μm, transport from their surfaces should be relatively unaffected by convection. A Sherwood number which retains a physically meaningful sense of a characteristic diffusion length is

$$Sh = \frac{k_L}{a_G D} \tag{11}$$

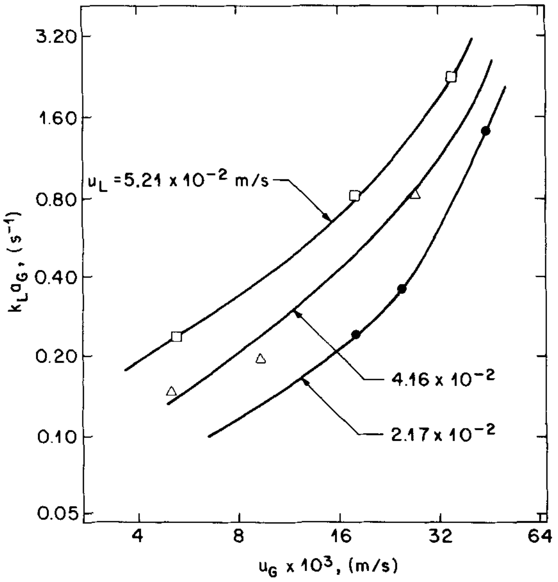

Figure 3. Gas-liquid mass transfer in the flow range $5.1 \times 10^{-3} < u_G < 5.1 \times 10^{-2}$ m/s and $2.1 \times 10^{-2} < u_L < 5.1 \times 10^{-2}$ m/s.

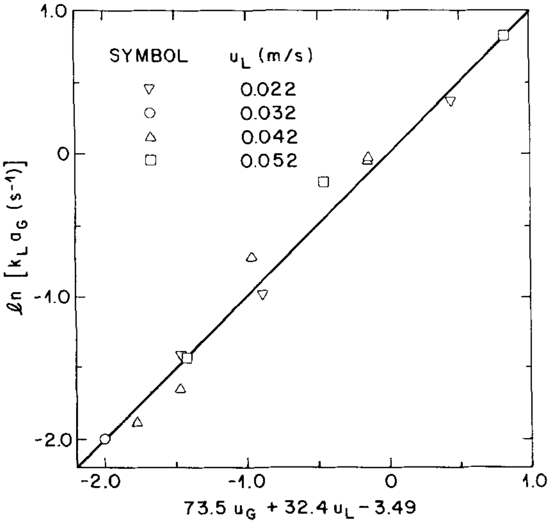

Figure 4. Gas-liquid mass transfer correlation.

where D is the reactant diffusivity in the liquid phase. For pure diffusion from uniform spherical bubbles,

$$Sh = \frac{2}{6\epsilon\beta_G} \tag{12}$$

If $\epsilon\beta_G$ is in the neighborhood of 0.3, $Sh = 1.1$ corresponds to pure diffusion. With use of Eqs. 7 and 10 over the range of mutual applicability, Sherwood numbers were plotted against gas areas, Figure 5. For high areas (small bubbles), the Sh indeed appears to approach an asymptotic value close to unity. Precise values of $\epsilon\beta_G$ are not known, and the actual bubbles are probably neither spherical nor monodisperse. However, Figure 5 suggests strongly that for the more vigorous flows, bubbles are very small and transport from them is controlled by diffusion, not convection.

While liquid velocities in this study were high, it is the liquid velocity with respect to the bubbles which affects mass transfer.

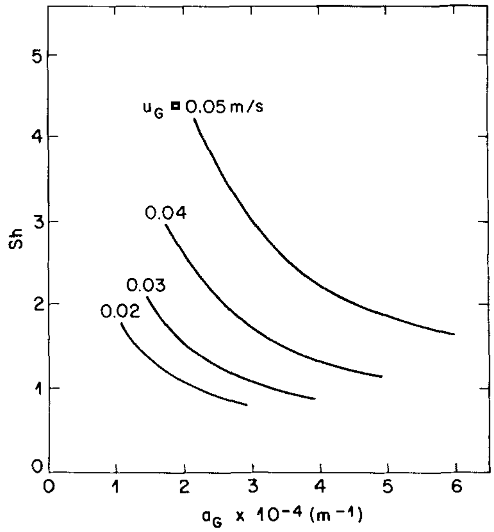

Figure 5. Gas-liquid Sherwood numbers, showing diffusion control in the high-area limit.

This relative velocity can arise from bouyant bubble rise, shearing forces of bubbles which pass close to the packing, and surface motion resulting from bubble breakup, coalescence, or shape instability.

Calderbank and Moo-Young (1961) studied mass transfer in bubble swarms, and considered that the flow around bubbles was caused primarily by bouyant lift. Under such circumstances, the balance between bubble rise and diffusion is described by the Rayleigh number,

$$Ra = \frac{d_b^3 \Delta \rho g}{\mu_L D} \tag{13}$$

Their experimental data confirmed that "small" bubbles moved as rigid spheres with no slip at their interface. As a result, their behavior

$$Sh_b = \frac{k_L d_b}{D} = 2.0 + 0.31\ Ra^{1/3} \tag{14}$$

was close to the theoretical relationship derived by Frossling, assuming that the drag coefficient was proportional to $Re^{-1/2}$. For small bubbles $Ra < 1$ and $Sh_b = 2.0$, which corresponds to pure diffusion. For aqueous systems, the bubble size at which the contribution of bouyant convection is comparable to that of pure diffusion is about 30 μm according to Eq. 14. This size is in the range of those calculated by Eq. 8 from the data of Figure 5, for which diffusion control is beginning to become evident.

For larger bubbles, surface velocities arising from the effects mentioned above result in significant convective mass transport effects. This is apparent from the data of Saada (1972), Voyer (1968), and Goto, who for the large bubbles of their systems, reported Sherwood numbers much greater than unity.

Conclusions

The gas-liquid specific surface areas measured in this study are as much as two orders of magnitude higher than values reported for other solutions and packing compositions. The difference is ascribed to the presence of electrolyte in the solution, and to the small size of the packing material. The results strongly suggest that in the small-particle regime of the present studies, interfacial effects are important, and that conventional scaling parameters (Re, Sc) are not sufficient to describe fluid flow and mass transfer. It is likely that both particle wetting and bubble-bubble interactions are important factors in the determination of gas-liquid flow patterns in small-particle packed beds.

The sodium sulfate solutions used in this study produced fine dispersions of small gas bubbles. The large surface areas which were observed are attributed to inhibition of bubble coalescence owing to the presence of the dissolved salt. Specific surface areas range from 4×10^3 to 2×10^5 m^{-1} for dispersed bubble flows. Bubble area is proportional to gas velocity. Liquid velocities have a pronounced effect on bubble size, with high velocities resulting in fine dispersions. The largest measured areas correspond to bubbles on the order of 10 μm, comparable in size to bubbles that are generated electrolytically.

Owing to the extensive surface areas, $k_L a_G$ values are high, and range from 0.1 to 2.3 s^{-1}. However, k_L values are low. The small bubbles are unlikely to break up or coalesce, and viscous drag prevents appreciable slip velocities. As a result, transport from the smallest bubbles is nearly diffusion controlled, with Sh values close to unity.

Acknowledgements

The authors wish to thank Mr. Brian Corey for assistance with experimental measurements. The work was funded in part by The American Chemical Society, ACS-PRF Grant #16437-7, 3C. Fellowship support was provided by Eastman Kodak Company.

Notation

a = specific surface area, m^{-1}
C = oxygen concentration, kmol/m^3
C^{sat} = local oxygen solubility in liquid, kmol/m^3
d = diameter, m
D = diffusivity, m^2/s
g = acceleration of gravity, m/s^2
k_r = second order rate constant, m^3/kmol · s
k_L = gas-liquid mass transfer coefficient, m/s
ℓ = packing length m
N = flux, kmol/m^2 · s
r_c = equilibrium concentration ratio, liquid/gas
Ra = Rayleigh number, $d_b^3 \Delta \rho g/\mu_L D$
Re = Reynolds number, $\rho_L u d_p/\mu_L$
Sh = modified Sherwood number, $k_L/(a_G D)$
Sh_b = bubble Sherwood number, $(k_L d_b)/D$
Sh_G = modified Sherwood number, $(k_L a_G d_p^2)/D$
u = superficial velocity, m/s

Greek letters

β_G = gas holdup, gas volume/void volume
ϵ = packing void fraction
μ = viscosity, kg/m · s
ρ = density, kg/m^3

Subscripts

0 = inlet
b = bubble
G = gas
ℓ = outlet
L = liquid
p = particle
t = tower

Literature Cited

Backstrom, H. L. J., "Der Kettenmekanismus bei der Autoxydation Von Natriumsulfitlosungen," *Z. Phys. Chem.*, **B25**, 122 (1934).

Battino, R., ed., "IUPAC Solubility Data Series: Oxygen and Ozone," 7, 152, Pergamon Press, Oxford (1981).

Brandon, N. P., G. H. Kelsall, S. Levine, and A. L. Smith, "Interfacial and Electrical Properties of Electrogenerated Bubbles," *J. Appl. Electrochem.*, **15**, 485 (1985).

Calderbank, P. H., and M. B. Moo-Young, "The Continuous Phase Heat and Mass Transfer Properties of Dispersions," *Chem. Eng. Sci.*, **16**, 39 (1961).

Charpentier, J. C., "Recent Progress in Two-Phase Gas-Liquid Mass Transfer in Packed Beds," *Chem. Eng. J.*, **11**, 161 (1976).

Charpentier, J. C., "Mass Transfer Rates in Gas-Liquid Absorbers and Reactors," *Adv. Chem. Eng.*, **11**, Academic Press, New York (1981).

Davis, R. E., G. L. Horvath, and C. W. Tobias, "The Solubility and Diffusion Coefficient of Oxygen in Potassium Hydroxide Solutions," *Electrochim. Acta*, **12**, 287 (1967).

de Waal, K. J. A., and J. C. Okeson, "The Oxidation of Aqueous Sodium Sulphite Solutions," *Chem. Eng. Sci.*, **21**, 559 (1966).

Ehdaie, S., M. Fleischmann, and R. E. W. Jansson, "Application of the Trickle Tower to Problems of Pollution Control: I. The Scavenging of Metal Ions," *J. Appl. Electrochem.*, **12**, 59 (1982).

Ellis, K. G., and R. E. W. Jansson, "The Indirect Electrochemical Epoxidation of Butenes and Ethylene in a Bipolar Trickle Tower," *J. Appl. Electrochem.*, **13**, 657 (1983).

Fukui, Y., and S. Yuu, "Removal of Colloidal Particles in Electroflotation," *AIChE J.*, **31**, 201 (1985).

Goto, S., J. Levec, and J. M. Smith, "Mass Transfer in Packed Beds with Two Phase Flow," *Ind. Eng. Chem. Proc. Des. Dev.*, **14**, 473 (1975).

———, "Trickle Bed Oxidation Reactors," *Cat. Rev. Sci. Eng.*, **15**, 187 (1977).

Hinze, J. O., "Fundamentals of the Hydrodynamic Mechanism of Splitting in Dispersion Processes," *AIChE J.*, **1**, 289 (1955).

Hofmann, H. P., "Multiphase Catalytic Packed Bed Reactors," *Cat. Rev. Sci. Eng.*, **17**, 71 (1978).

Lessard, R. R., and S. A. Zieminski, "Bubble Coalescence and Gas Transfer in Aqueous Electrolyte Solutions," *Ind. Eng. Chem. Fund.*, **10**, 261 (1971).

Linek, V., and J. Mayrohoferova, "The Kinetics of Oxidation of Aqueous Sodium Sulfite Solutions," *Chem. Eng. Sci.*, **25**, 787 (1970).

Lister, A., "Engineering Design and Development of Desulphurizer Reactors," *Proc. Eur. Symp. Chem. React. Eng.*, Pergamon Press, London, 225 (1964).

Miller, C. A., "Stability of Interfaces," *Surface and Colloid Science*, **10**, 227, Plenum Press, New York (1978).

Ohshima, S., T. Takematsu, Y. Kuriki, K. Shimada, M. Suzuki, and J. Kato, "Liquid Phase Mass Transfer Coefficients and Gas Hold Up in a Packed Bed Concurrent Upflow Column," *J. Chem. Eng. Japan*, **9**, 29 (1976).

Oloman, C., and A. P. Watkinson, "Electrolyte Production of Alkaline Peroxide Solutions," U.S. Pat. 3,969,201 (July, 1976).

Oloman, C., and A. P. Watkinson, "Hydrogen Peroxide Production in Trickle Bed Electrochemical Reactors," *J. Appl. Electrochem.*, **9**, 117 (1979).

Saada, M. Y., "Assessment of Interfacial Area in Co-Current Two-Phase Flow in Packed Beds," *Chim. Ind. Gen. Chim.*, **105**, 1415 (1972).

Sweed, N. H., "Intraparticle and Interphase Transport Resistances in Gas-Liquid-Solid Catalytic Reactors," *NATO Adv. Study Inst. Ser.*, **52**(E), (Multiphase Chem. React., v. 2, 135 (1981).

Takahashi, K., and R. Alkire, "Mass Transfer in Gas Sparged Porous Electrodes," *Chem. Eng. Commun.*, **38**, 209 (1985).

Takahashi, K., "Homogeneous Catalysis in Flow-by Porous Electrodes Containing Gas-Liquid Flow," Ph.D. Thesis, Univ. of Illinois, Urbana (1986).

van Deemter, J. J., "Trickle Hydrodesulfurization—A Case History," *Proc. Eur. Symp. Chem. React. Eng.*, Pergamon Press, London, 215 (1964).

Vogel, A. I., *Quantitative Inorganic Analysis*, 3rd ed., Longman, London (1961).

Voyer, R. D., and A. I. Miller, "Improved Gas-Liquid Contacting in Concurrent Flow," *Can. J. Chem. Eng.*, **46**, 335 (1968).

Zieminski, S. A., and R. C. Whittemore, "The Behavior of Gas Bubbles in Aqueous Electrolyte Solution," *Chem. Eng. Sci.*, **26**, 509 (1971).

Manuscript received Dec. 8, 1986, and revision received Apr. 29, 1988.